

Article

PV-Powered Charging Station with Energy Cost Optimization via V2G Services

Saleh Cheikh-Mohamad, Berk Celik *, Manuela Sechilariu  and Fabrice Locment 

AVENUES, Université de Technologie de Compiègne, Centre Pierre Guillaumat-CS 60 319, 60203 Compiègne, France; saleh.cheikh-mohamad@utc.fr (S.C.-M.); manuela.sechilariu@utc.fr (M.S.); fabrice.locment@utc.fr (F.L.)

* Correspondence: berk.celik@utc.fr; Tel.: +33-(0)3-44-23-44-06

Featured Application: This article presents a mixed-integer linear programming optimization problem to minimize the energy cost of a charging station powered by photovoltaics via V2G service.

Abstract: Satisfying the increased power demand of electric vehicles (EVs) charged by clean energy sources will become an important aspect that impacts the sustainability and the carbon emissions of the smart grid. A photovoltaic (PV)-powered charging station (PVCS) formed by PV modules and a stationary storage system with a public grid connection can provide cost-efficient and reliable charging strategies for EV batteries. Moreover, the utilization of vehicle-to-grid (V2G) service is a promising solution, as EVs spend most of their time idle in charging stations. As a result, V2G services have the potential to provide advantages to both public grid operators and EV users. In this paper, an energy management algorithm of a PVCS formulated with mixed-integer linear programming is presented to minimize the total energy cost of the participation of EV users in V2G service. Simulation results demonstrate that the proposed optimization method satisfies EV user demands while providing V2G service and highlights the benefits of the V2G service where the determined costs of the proposed algorithm perform significantly better compared to the baseline scenario (simulation without optimization).

Keywords: charging station; electric vehicle; energy cost optimization; photovoltaic; vehicle-to-grid



Citation: Cheikh-Mohamad, S.; Celik, B.; Sechilariu, M.; Locment, F.

PV-Powered Charging Station with Energy Cost Optimization via V2G Services. *Appl. Sci.* **2023**, *13*, 5627. <https://doi.org/10.3390/app13095627>

Academic Editor: Frede Blaabjerg

Received: 29 March 2023

Revised: 24 April 2023

Accepted: 28 April 2023

Published: 3 May 2023



Copyright: © 2023 by the authors. Licensee MDPI, Basel, Switzerland. This article is an open access article distributed under the terms and conditions of the Creative Commons Attribution (CC BY) license (<https://creativecommons.org/licenses/by/4.0/>).

1. Introduction

Photovoltaic (PV)-powered charging stations (PVCS) are designed for charging electric vehicles (EV) using clean energy sources that can be installed on car parking shades and/or building rooftops. Charging EVs with renewable energy sources, particularly PV sources, is a crucial factor in enhancing their environmental benefits and reducing their greenhouse gas emissions [1]. To achieve defined objectives such as minimizing charging costs and providing a satisfactory charging process for EV users [2], it is necessary to implement an energy management system that can control and monitor the energy flows within the PVCS. A feasibility study of a PVCS has been conducted by analyzing its effectiveness based on technical, economic, and environmental aspects by comparing the impact of different geographical areas on the installation location in [3]. The study investigates how a PVCS can contribute to charging EVs with different energy mixes and compares the produced CO₂ emissions of charging EV batteries solely from the grid, from the PVCS, and with internal combustion engine vehicles. They have found that the PVCS concept is more efficient in countries with high annual average irradiance and significant CO₂ emissions in their grid, but it remains economically unfeasible due to expensive storage systems. In [4], a supervision control system is presented for smart charging of an EV fleet in a PVCS-based research building. The proposed control strategy is based on a real-time operation to satisfy EV users using PV forecasting and EV charging historical records over four years to predict

the EV power profiles. A user-friendly smart charging method, which includes interactions with EV users via an interface, has been developed in [5], where the EV user is a key player in the process of choosing the best scenario among uncoordinated charging, smart charging, and bidirectional smart charging control in a PVCS. The proposed methodology is based on real-time rule-based control and a predictive linear optimization control. The results showed that bidirectional charging control had the best cost reduction, while uncoordinated charging control costs the most. In [6], mixed-integer programming was investigated to minimize the cost of energy traded to a PVCS, where the intermittency of PV power can be compensated by EVs which can also discharge energy to the PVCS, where it does not integrate stationary storage. The EVs are classed in three categories according to their charging behavior, and the results showed that an increase of green EVs, the only category of EVs for which the users can allow discharging of energy into the charging station, could reduce the total cost of the PVCS. In [7], mixed-integer linear programming (MILP) has been applied to optimize the sizing of a PVCS components (PV, stationary storage, and transformer) in order to minimize the investment cost and the total cost considering the uncertainties of PV and EV charging power profiles. The simulation results, with a 1-h step time, showed that EV charging stations powered by PV are more cost-effective than EV charging stations powered by the grid.

However, large-scale EV charging will pose difficulties from a power point of view for grid operators [8]. Therefore, charging of EVs should be controlled intelligently in order to reduce the negative impact on the connected public grid [9]. Additionally, EVs remain in an idle state for a long time. As a result, they can serve as energy storage systems and assist the grid by providing energy when they are plugged in. In this way, EVs can be charged during off-peak periods and discharged during peak periods to support the public grid and/or a microgrid. This approach enables EVs to be utilized as a flexible load, with their charging and discharging being controlled. Therefore, vehicle-to-grid (V2G) services have emerged as a promising technology in the field of smart grids [10], where they can improve frequency [11] and voltage regulations while providing benefits to the EV users [12], and this depends on the number of available EVs [13,14]. Additionally, such services can enhance power quality and promote the integration of renewable energy with developed smart control algorithms [15–17]. In [18], the benefits are highlighted for V2G service participants, as these services can decrease the total ownership cost of EVs. For the grid operator, V2G is seen as a power source that is able to mitigate fluctuations caused by renewable energy sources and provide ancillary services. As for EV owners, participating in V2G services should have financial incentives without limiting their travel needs.

Moreover, V2G optimization plays a crucial role in maximizing the benefits. In [19], the authors found that total cost of EV ownership could be reduced by implementing V2G service in the Flanders region of Belgium. This service helped to smooth out electricity demand by filling in valleys and reducing power peaks, ultimately leading to improved grid stability. A charging and discharging strategy for EVs proving the effectiveness of their V2G operation in different cities in China with different trip patterns was developed in [20]. Their aim was to minimize the cost of operation of the distribution grid considering grid congestion and voltage constraints. These factors were particularly important, given the variation in the distribution of EVs across areas of operations. The potential locations for EV charging and their participation in V2G service have been predicted in [21] using automated machine learning, based on historical data collected over 42 weeks. The authors of [22] have demonstrated that the participation of EVs in V2G services, when they are idle at charging stations, can reduce the demand for charging EVs. In [23], an improved harmony particle swarm optimization problem was investigated in a bi-level model (low level: EV cluster scheduling, upper level: planning) to determine the optimal allocation of distributed generation and charging stations within a V2G service. The results indicated that the optimized model could satisfy the charging demand of EV users, improve the voltage quality, mitigate load fluctuations, encourage the use of renewable energy, and improve the global performance of the planning scheme. An optimization framework has

been developed in [24] to reduce greenhouse gases and intensive electricity imports in the Switzerland power system with controlled charging/discharging of EVs. To jointly install EV charging stations and distributed energy resources in a distribution system in China, an optimization model has been presented in [25], where V2G service is considered with minimized annual costs (considering also social aspects). An optimization problem has been modeled in [26] as a nonlinear stochastic programming problem with uncertainty of PV energy. The EVs can operate in V2G mode, where this allows EVs to charge during off-peak hours and discharge during peak hours to reduce energy costs. The proposed problem can optimize the operation of EVs and minimize the cycles of their batteries to reduce battery degradation speed. A novel control system has been presented in [27] to underpin V2G service by deploying a fleet of EVs, which allows a V2G aggregator to provide voltage and frequency services while reducing the charging cost with the minimization of battery-level degradation. A case study of an EV charging station based on a university campus in Jordan has been presented in [28], which investigates the feasibility of a V2G service to minimize the global consumption of energy drawn from the public grid. A computational model of an EV with battery degradation has been studied in [29] to supply power to the grid while gaining profit for the EV owner by alleviating the load on the main grid. The results show that the potential benefits from V2G are greater than the cost of battery degradation.

On the other hand, research studies have investigated the optimization of V2G service in a PVCS. In [30], a dynamic searching peak-and-valley algorithm was proposed to determine the optimal charging and discharging start time of EVs based on their initial state-of-charge (SOC), arrival time, charging mode, departure time, and the tariffs in peak hours. The aim of this optimization was to reduce the burden on the public grid and lower its energy cost. A control scheme using a grid-connected inverter was developed in [31] to improve the voltage and frequency stability of a PVCS with V2G operation. This inverter can identify unusual faults of the microgrid and functions in islanding mode. The authors in [32], have modeled a PVCS to provide ancillary services where EV users can receive rewards for their V2G participation. The results proved that EVs participating in V2G service could provide high availability of service. Furthermore, in [33], an energy management strategy has been examined for the real-time control of multi-source EV charging to lower the operating cost, taking into consideration battery degradation of stationary storage and EVs for their V2G participation. In [34], a PVCS was designed with V2G service to lower the stress on the public grid and to enhance its stability during peak hours. The authors also discussed possible financial incentives that can motivate EV users to participate in the demand response. Additionally, an energy management and control system has been introduced in [35] for an EV charging station with V2G integration. This charging station featured a PV system, wind turbine, and fuel cell with grid connection. A MILP model has been proposed in [36] for a parking lot of EVs powered with a microgrid, based on PV sources, wind turbines, hydrogen energy, and a stationary storage system to minimize the total sustainability cost, as well as economic and environmental costs. The EVs can operate in V2G mode to participate in demand response, thus encouraging EV users to charge in off-peak periods instead of on-peak periods. In [37], a day-ahead operation planning method that incorporates EVs with V2G service in a microgrid was investigated to minimize the daily operation costs. A multi-objective optimization model has been proposed in [38] for a microgrid integrating EVs with V2G service. Their objectives were maximizing the use of renewable energy, maximizing the benefits for EV users, and minimizing grid load fluctuation. A heuristic optimization problem has been studied in [39] to optimize the sizing of a hybrid PV sources, battery, and diesel generator for an EV parking lot with V2G service, where EVs are considered as a flexible load. A two-stage smart charging algorithm (first stage: optimization problem, second stage: real-time control) has been proposed in [40] for buildings integrating EVs, PV sources, a storage system, and a heat pump. The optimization problem is formulated as a non-linear programming model to optimize the operation of EVs. The results show the benefits of V2G service as primary frequency regulation reserve while participants achieve energy cost reductions; however,

the degradation of Li ion batteries is non-negligible. The authors in [41] have proposed an effective strategy using adjustable robust optimization to enhance the operation stability and economic cost of a microgrid by enabling V2G service during peak periods and charging for valley filling at off-peak periods to minimize the cost of operation under various constraints.

The references cited earlier have highlighted the role of V2G in serving as a spinning reserve source and power regulation to lower the impact of the peak load on the grid and its associated services. Yet, their optimization problems are mostly based on day-ahead prediction of EV profiles modeled with a probability distribution function, whereas the proposed optimization algorithm in this paper is actualized at every arrival of a new EV, considering the impact of the uncertainties in real-time simulation. This paper is an extension of [42], where V2G is realized with a rule-based control scheme, whereas in this extended version, the focus is on the energy cost optimization problem with V2G implementation in the PVCS. In this paper, a PVCS with five chargers that can support three charging modes, slow, average, and fast charging, is presented. The PVCS combines PV sources, a stationary storage system, a public grid connection, and EVs as a flexible load that can operate in V2G mode. The human-machine interface (HMI) allows the EV users to interact with the PVCS and choose their preferences, such as charging mode, desired state of charge SOC at departure, and willingness to participate in V2G service. Additionally, EV users arrive arbitrarily at the PVCS, and their arrivals are unpredictable. In [43], the authors presented a control mechanism aimed at minimizing the discomfort of EV users for a charging station equipped with PV sources and connected to a public grid, but without a stationary storage system. However, their study differs from ours in several ways. Firstly, they only allow for one charging mode, namely the slow mode, whereas we offer three different charging modes. Secondly, their focus is on maximizing social welfare and minimizing the discomfort of EV users, while the objective in this study is to minimize the total energy cost of the PVCS, with optimization being updated for each EV arrival. Furthermore, the energy injected into the grid from EVs and the energy distribution for each EV charging from each power source are being analyzed to provide a more comprehensive understanding of the system's energy dynamics. To sum up, the main contributions of this paper are:

1. Proposing an energy cost optimization problem in a PVCS with V2G service, taking into consideration the uncertainty of the arrival time of EVs in a real-time simulation;
2. Actualizing the optimization problem formulated via MILP at every arrival of a new EV; the arrival of EVs is not modeled based on day-ahead prediction; instead it is randomly generated as unpredicted events in MATLAB;
3. Assessing the energy consumption of every EV from each power source and the energy participation among the power sources (PV, energy storage, and grid).

The paper is organized as follows: Section 2 introduces the PVCS with V2G energy cost optimization. Section 3 develops the energy cost optimization problem. Section 4 describes the different simulation cases with V2G service. Section 5 analyzes the energy cost results. Section 6 concludes the paper.

2. PV-Powered Charging Station with V2G Service

The PVCS infrastructure consists of PV modules, a stationary storage system, and a connection with the public grid [42], as illustrated in Figure 1.

In Figure 1, p_{PV_MPPT} is the PV power operating in maximum-power point-tracking (MPPT) mode, p_{PV} is the PV power after shedding (if it is necessary), p_{G_I} is the power injection into the public grid, p_{G_S} is the power supply from the public grid, p_{S_C} is the charging power of the stationary storage, p_{S_D} is the discharging power of the stationary storage, p_{PVCS_D} is the total demand power of EVs, and p_{PVCS} is the total charging power of EVs after shedding (if it is necessary). The PVCS is designed such that the public grid can provide power to charge EVs and also absorb power in case of excess energy from PV sources or discharging EVs. Each component of the PVCS is connected to the DC bus using

dedicated converters. The EVs' batteries are considered as controllable loads because they can be charged or discharged at variable or constant power. To ensure a consistent power supply and reduce the difference between power production and load, the public grid connection is formed through a bidirectional AC/DC converter. The stationary storage is charged solely by PV sources and can be discharged to provide power for EVs' load.

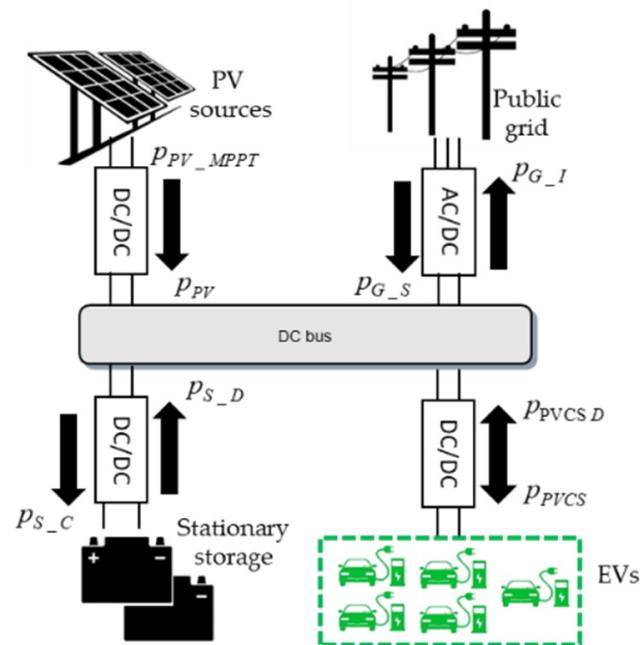


Figure 1. Scheme of PV-powered charging station with V2G service.

2.1. PV-Powered Charging Station with V2G Service without Energy Cost Optimization

The PVCS can operate without energy cost optimization based on the storage priority algorithm shown in Figure 2. In this case, the EVs are charged using PV sources first, followed by the stationary storage system, and finally by the public grid. The surplus PV production is used to charge the stationary storage system. However, if the storage system has reached its capacity or charging power limit and there is still unused excess PV power, the remaining power is injected into the public grid. Participating in a V2G service allows EV users to discharge their EVs for up to 15 min or until the battery is fully discharged during peak periods. Following the V2G operation, the EVs will then be charged to achieve the desired SOC at departure. The charging can be performed using any available power, regardless of the initial charging mode, as long as the charging terminal can support variable power up to 50 kW.

2.2. PV-Powered Charging Station with V2G Service with Energy Cost Optimization

On the other hand, the PVCS can operate with energy cost optimization. In this case, Figure 3 describes the supervisory control system for the PVCS [44]. The supervisory control system of the PVCS is composed of four layers: prediction, energy cost optimization, operation, and HMI. The control block has been designed and implemented to interact with EV users and maintain power balance at the DC bus through the energy cost optimization and operation layers.

The prediction layer utilizes weather forecasts. From the interaction with the HMI, the user of an EV v selects their desired SOC at departure charging mode, participates in the V2G service, and obtains the SOC of their EV at arrival in real-time. The energy cost optimization relies on the production prediction, which depends on the hourly solar irradiation predictions and consumption profile communicated from the HMI. Moreover, the power limits of the connected public grid, energy pricing, and energy system limits

are communicated. The MILP formulation is used to reduce the total energy cost of the PVCS. This supervisory control system has the advantage of interacting with EV users for optimization; yet, if the choices of the EV users are not practical, they must be adjusted in order to enable optimization [45]. For instance, if an EV user arrives at the charging station and requests fast charging, but the available power cannot support it, the HMI will communicate with the user to suggest charging in average or slow mode, waiting for available power, or leaving the charging station altogether. Similarly, if the EV user mistakenly inputs an invalid SOC at departure (e.g., 180%), the HMI will alert the user to enter a valid SOC interval below 100%. Whenever a new EV arrives, the optimization process is updated with the new inputs from the HMI and physical constraints. Therefore, the process is repeated each time a new EV arrives.

Dealing with the unpredicted arrival of EVs is the main challenge. The power references for the public grid, stationary storage, and EVs are sent to the operation layer based on the optimization results. The operation layer is responsible for maintaining the power balance while respecting the system’s constraints and physical limitations [46]; furthermore, it sets the PV power limitation and applies EV shedding if needed.

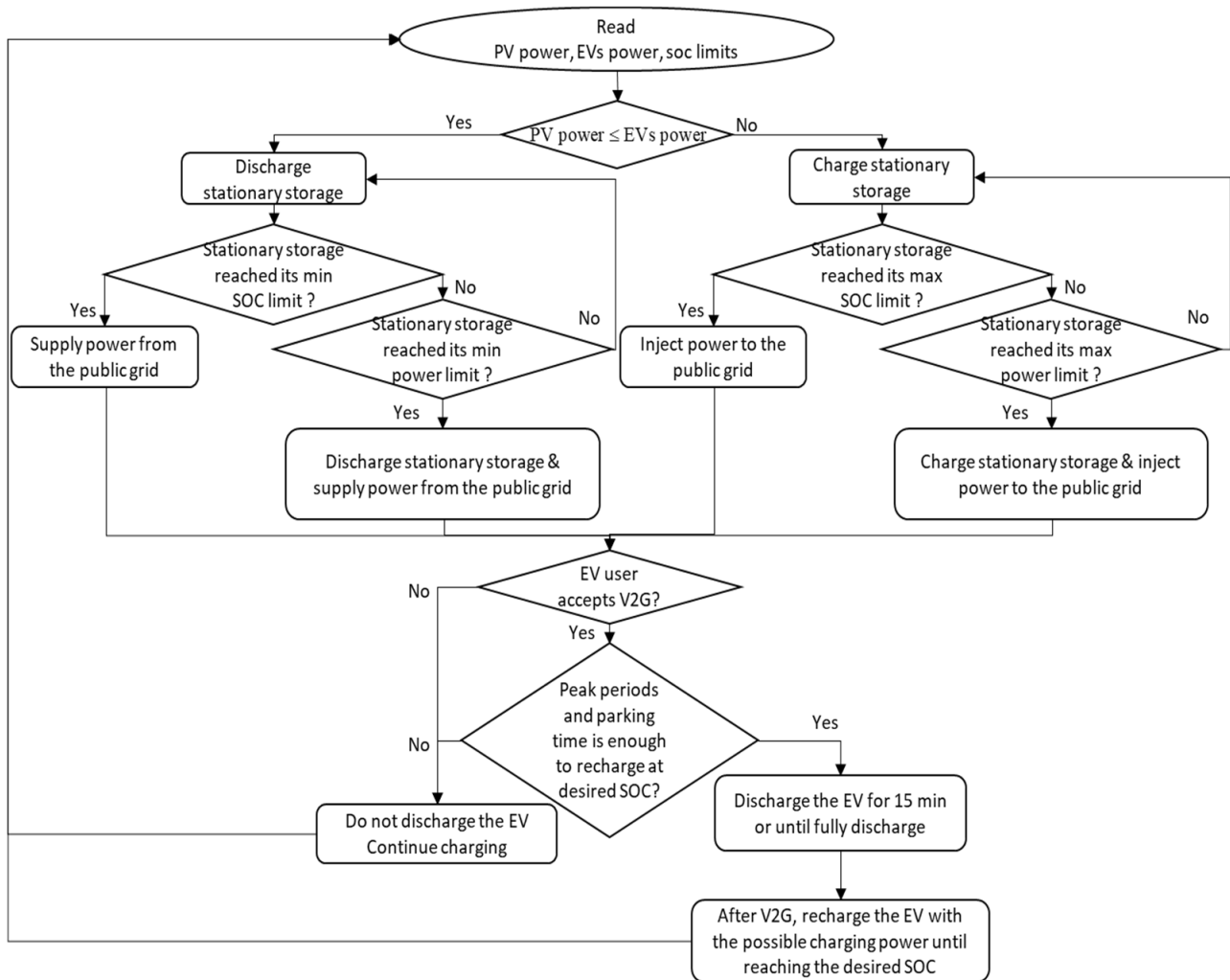


Figure 2. PV-powered charging station energy management via V2G service without optimization.

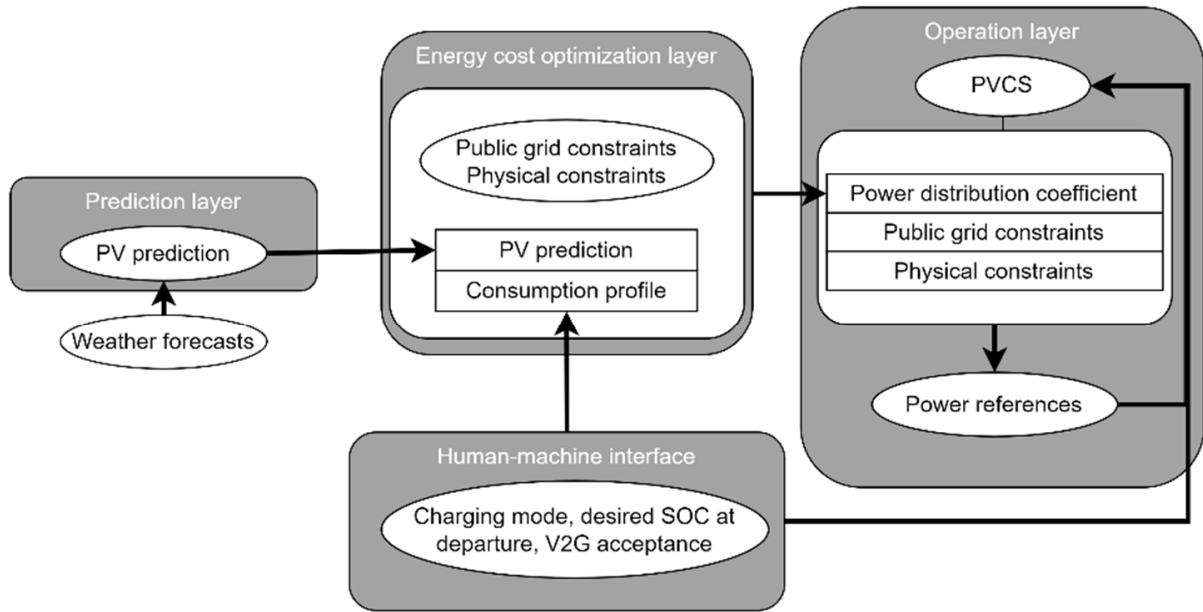


Figure 3. Supervisory control system for the PVCS [44].

2.2.1. Prediction Layer

In the prediction layer, hourly solar irradiation predictions are provided by Météo France to calculate the PV power prediction. The PV power prediction is based on solar irradiation (g) and the ambient temperature (T_{amb}) from forecasted data [47]. Therefore, the PV power prediction $p_{PV_MPPT_pred}$ is calculated in MPPT mode for each time instant t_i [48] as in Equations (1) and (2), and it is introduced into the energy cost optimization layer:

$$p_{PV_MPPT_pred}(t_i) = P_{PV_STC} \cdot \frac{g(t_i)}{1000} \cdot [1 + \gamma \cdot (T_{PV}(t_i) - 25)] \cdot N_{PV} \text{ with } t_i = \{t_0, t_0 + \Delta t, t_0 + 2\Delta t, \dots, t_F\}, \quad (1)$$

$$T_{PV}(t_i) = T_{amb}(t_i) + g(t_i) \cdot (NOCT - T_{air-test}) / G_{test}, \quad (2)$$

where P_{PV_STC} is the PV power in standard test conditions (STC), γ is the power coefficient of temperature ($-0.29\%/^{\circ}\text{C}$), N_{PV} is the number of PV panels, T_{PV} is the PV cell temperature, and t_0 , Δt , and t_F are the initial time instant, time interval between two samples, and time instant at the end of operation, respectively. $NOCT$ is the nominal operating cell temperature (41°C), G_{test} is the fixed solar irradiation (800 W/m^2), and $T_{air-test}$ is the fixed air temperature (20°C).

2.2.2. Human–Machine Interface

This layer interacts with the EV users, allowing them to choose their preferred charging mode M_v among slow, average, and fast. It should be noted that all EVs have the same energy capacity and can handle fast charging. The HMI obtains the SOC of the EVs at their arrivals $SOC_{EV_arr_v}$ and assists the users in selecting their desired SOC at departure $SOC_{EV_des_v}$, as well as their participation in V2G service $V2G_{EV}$ in real-time. Therefore, the estimated charging time $t_{est_ch_v}$, which indicates the time required to reach the desired SOC, is determined in Equation (3):

$$t_{est_ch_v} = (SOC_{EV_des_v} - SOC_{EV_arr_v}) \cdot E / P_{EV_max_v}, \quad (3)$$

where E is the EV battery capacity, and $P_{EV_max_v}$ is the maximum power of EV charging based on the charging mode selected by the user. The HMI for the PVCS is explained thoroughly in [49], and once the user preferences are set in the HMI, these data are communicated simultaneously to the operation layer and to the energy cost optimization layer to actualize the optimization with these data.

2.2.3. Energy Cost Optimization

This layer interacts with the prediction layer and the HMI to carry out the optimization to minimize the total energy cost. This layer, the power references for the stationary storage, the public grid, and the EVs, which are the decision variables, are sent to the operational layer. The optimization has several benefits, such as minimizing the energy cost, determining the optimal contribution of the stationary storage or the public grid, and avoiding EV and PV shedding. The energy pricing is considered for on-peak and off-periods with fixed tariffs, and the limits for public grid power injection and supply are defined with the public grid operators. Moreover, the physical limitations of the stationary storage should be respected to avoid its damage. The energy cost optimization problem is detailed in Section 3.

2.2.4. Operation Layer

From the energy optimization layer, the optimal power flow for the sources and the EVs considering $p_{PV_MPPT_pred}$ and p_{PVCS} is found. The optimized powers for the stationary storage and the public grid are obtained through the optimization layer. However, these optimized powers are not sent directly into the operation layer. Instead, the power distribution coefficient k_D is identified and introduced into the operation layer to account for uncertainties in the forecasted data. The power distribution coefficient k_D determines the power share between the public grid and the stationary storage. Thus, if PV power is insufficient for EV charging, either the public grid or the stationary storage or both can continue supplying power to charge the EVs based on the value of k_D (see Section 5). The upside of k_D is coupling easily the energy management with the operation layer while respecting all constraints [47].

The operation layer must ensure robustness and be able to withstand uncertainties in the forecast data. After that, this layer defines the power references and applies PV or EV shedding when needed. To maintain the DC bus at the reference voltage V_{ref} , the actual operating conditions are used to determine the power reference p_{ref} using Equations (4) and (5):

$$p_{ref}(t_i) = p_{PV}(t_i) - p_{PVCS_D}(t_i) - C_P(V_{ref} - v_{DC\ bus}), \quad (4)$$

$$p_{ref}(t_i) = p_{G_ref}(t_i) + p_{S_ref}(t_i), \quad (5)$$

where C_P is the proportional controller gain, and $v_{DC\ bus}$ is the actual voltage of the DC bus. The power reference for the public grid p_{G_ref} and the stationary storage p_{S_ref} can be obtained by (6), and the power distribution coefficient k_D is given by (7):

$$p_{S_ref}(t_i) = k_D(t_i) \cdot p_{ref}(t_i), \quad (6)$$

$$k_D(t_i) = \frac{p_{S_C}(t_i) + p_{S_D}(t_i)}{p_{S_C}(t_i) + p_{S_D}(t_i) + p_{G_I}(t_i) + p_{G_S}(t_i)} \text{ with } k_D \in [0, 1]. \quad (7)$$

3. Energy Cost Optimization with V2G Service

The principal objective of the formulated optimization problem is to minimize the total energy cost while satisfying various constraints [47]. The constraints and objective function are explained in detail in the following subsections.

3.1. PV Sources

PV system can operate in two modes: MPPT or limited-power mode. The latter mode is used in case of excessive surplus PV production which exceeds the total EV load, the allowed stationary storage charging power, and the public grid injection power. In the MPPT mode, there is no need to shed any PV power, and thus PV shedding p_{PV_S} is zero. However, in the power-limitation mode, p_{PV_S} becomes positive, indicating the amount of PV power that needs to be shed to ensure that the total power injected into the grid does

not exceed the limits. Accordingly, p_{PV} is calculated [47] as given by (8) with the constraint of p_{PV_S} in (9) and (10):

$$p_{PV}(t_i) = p_{PV_MPPT}(t_i) - p_{PV_S}(t_i), \tag{8}$$

$$p_{PV}(t_i) \geq 0, \tag{9}$$

$$0 \leq p_{PV_S}(t_i) \leq p_{PV_MPPT}(t_i). \tag{10}$$

3.2. Stationary Storage

In order to extend the lifetime of the lithium-ion batteries as a stationary storage method and protect them from overcharging or over-discharging, the maximum and minimum SOC of the storage, SOC_{S_max} , SOC_{S_min} , as well as the maximum storage power P_{S_max} must be respected as given by (11) and (12) [47,50]. The SOC of the storage soc_S can be simplified as in [51], neglecting the effects of self-discharge and temperature, and is given by (13) below:

$$-P_{S_max} \leq p_S(t_i) \leq P_{S_max}, \text{ where } p_S(t_i) = p_{S_C}(t_i) - p_{S_D}(t_i), \tag{11}$$

$$SOC_{S_min} \leq soc_S(t_i) \leq SOC_{S_max}, \tag{12}$$

$$soc_S(t_i) = SOC(t_0) + \frac{1}{3600 \cdot E_{Bat}} \int_{t_0}^t p_S(t_i) dt, \tag{13}$$

where E_{Bat} and p_S are the energy capacity (kWh) and power of the stationary storage, respectively.

3.3. Grid Connection

The maximum limits for the grid supply and injection $P_{G_S_max}$ and $P_{G_I_max}$, set by the public grid, should be respected [47], as given by (14), where p_G is the public grid power:

$$-P_{G_S_max} \leq p_G(t_i) \leq P_{G_I_max}, \text{ where } p_G(t_i) = p_{G_I}(t_i) - p_{G_S}(t_i). \tag{14}$$

3.4. Electric Vehicles

When the stationary storage and public grid have reached their limits, it may not be possible to fully supply EV batteries, which represent the entire load of the PVCS. In such cases, the charging of EVs can be shed [47]. Moreover, it should be noted that p_{PVCS} can be negative when an EV is in the process of discharging into the grid during V2G service. In situations where there is enough PV power available, there is no need to shed any PV production. Similarly, when there is sufficient charging capacity available, there is no need to shed any EV charging power. Moreover, the stationary storage could be charged, and/or the public grid could absorb power when PV production is higher than load demand. On the other hand, when the load demand exceeds the PV production, the stationary storage can be discharged, and/or the public grid can supply power. Therefore, the constraints given by (15) and (16) must be respected.

$$\text{if } p_{PV_MPPT}(t_i) \geq p_{PVCS_D}(t_i) \text{ then } \begin{cases} p_G(t_i) \geq 0 \\ p_S(t_i) \geq 0 \end{cases}, \tag{15}$$

$$\text{if } p_{PV_MPPT}(t_i) \leq p_{PVCS_D}(t_i) \text{ then } \begin{cases} p_{PV_S}(t_i) = 0 \\ p_G(t_i) \leq 0 \\ p_S(t_i) \leq 0 \end{cases}. \tag{16}$$

The PVCS interface allows EV users to make choices regarding their charging mode and other preferences. The constraints given in (17)–(34) reflect the interaction between EV users and the supervisory control system.

3.4.1. V2G Mode

The following constraints given below in (17)–(23) are included in the optimization problem for the EV users who accept providing V2G services.

$$disch_min \cdot 60 / \Delta t \leq \sum V2G_{bin_v}(t_i) \leq disch_max \cdot 60 / \Delta t \quad \forall t_i \in [t_{arr_v}, t_{dep_v}] \quad (17)$$

$$V2G_{SW_v}(t_i) \geq V2G_{bin_v}(t_i) - V2G_{bin_v}(t_{i-1}) \quad \forall t_i \in [t_{arr_v}, t_{dep_v}] \quad (18)$$

$$G2V_{SW_v}(t_i) \geq G2V_{bin_v}(t_i) - G2V_{bin_v}(t_{i-1}) \quad \forall t_i \in [t_{arr_v}, t_{dep_v}] \quad (19)$$

$$G2V_{bin_v}(t_i) + V2G_{bin_v}(t_i) \leq 1 \quad \forall t_i \in [t_{arr_v}, t_{dep_v}] \quad (20)$$

$$-P_{EV_fast_max} \cdot V2G_{bin_v}(t_i) \leq p_{EV_v}(t_i) \quad \forall t_i \in [t_{arr_v}, t_{dep_v}] \quad (21)$$

$$p_{EV_v}(t_i) \leq P_{EV_fast_max} \cdot G2V_{bin_v}(t_i) \quad \forall t_i \in [t_{arr_v}, t_{dep_v}] \quad (22)$$

$$p_{EV_v}(t_i) - p_{EV_v}(t_{i-1}) \leq Limit \cdot \Delta t / 60 \cdot G2V_{bin_v}(t_i) \quad \forall t_i \in [t_{arr_v}, t_{dep_v}] \quad (23)$$

where *disch_min* (5 min) and *disch_max* (15 min) are the minimum and maximum duration for the EV's discharge, while *t_{arr_v}* and *t_{dep_v}* are the time of arrival and departure of vehicle *v*, respectively. *G2V_{bin_v}* and *V2G_{bin_v}* are binary decision variables for charging/discharging times; *G2V_{SW_v}* and *V2G_{SW_v}* are binary decision variables for the switching times between charging/stop and discharging/stop; *p_{EV_v}* is the EV charging power of vehicle *v*; *P_{EV_fast_max}* is the fast charging power at maximum; and *Limit* is the ramp-up charging power (15 kW/min). Constraint (17) determines the discharging period of the EV, while Constraints (18) and (19) determine that the discharging and charging times of the EV, respectively, should be successive. Constraint (20) specifies that the EV can either charge, discharge, or be idle at any given time. Constraints (21) and (22) refer to the discharging and charging power of the EV, respectively. Lastly, Constraint (23) helps to reduce the charging fluctuations of the EV.

3.4.2. EV Charging Mode

If the EV user does not want to participate in the V2G service, Constraints (24)–(27) are used for charging the EV battery, where the charging power is determined by the charging mode selected by the EV user as follows:

$$if M_v = 1 then 0 \leq p_{EV_v}(t_i) \leq P_{EV_fast_max} \quad \forall t_i \in [t_{arr_v}, t_{dep_v}] \quad with v = \{1, 2, \dots, N_v\}, \quad (24)$$

$$if M_v = 2 then 0 \leq p_{EV_v}(t_i) \leq P_{EV_aver_max} \quad \forall t_i \in [t_{arr_v}, t_{dep_v}], \quad (25)$$

$$if M_v = 3 then 0 \leq p_{EV_v}(t_i) \leq P_{EV_slow_max} \quad \forall t_i \in [t_{arr_v}, t_{dep_v}], \quad (26)$$

$$p_{EV_v}(t_i) = 0 \quad \forall t_i \notin [t_{arr_v}, t_{dep_v}], \quad (27)$$

where *N_v* is the total number of EVs, *P_{EV_aver_max}* is the average charging power at maximum, and *P_{EV_slow_max}* is the slow charging power at maximum. The total EV charging power in (28) and the SOC calculation with its constraints in (29)–(34) are given:

$$p_{PVCS}(t_i) = \sum_v^{N_v} p_{EV_v}(t_i) \quad \forall t_i \in [t_{arr_v}, t_{dep_v}], \quad (28)$$

$$SOC_{EV_min} \leq soc_{EV_v}(t_i) \leq SOC_{EV_max} \quad \forall t_i \in [t_{arr_v}, t_{dep_v}], \quad (29)$$

$$soc_{EV_v}(t_i) = 0 \quad \forall t_i \notin [t_{arr_v}, t_{dep_v}], \quad (30)$$

$$soc_{EV_v}(t_i) = SOC_{EV_arr_v}(t_i) \quad \forall t_i = t_{arr_v}, \quad (31)$$

$$SOC_{EV_arr_v}(t_i) \geq SOC_{EV_min} \quad \forall t_i = t_{arr_v} \quad (32)$$

$$soc_{EV_v}(t_{i+1}) = soc_{EV_arr_v}(t_i) + \frac{1}{3600 \cdot E} \int_{t_{arr_v}}^{t_{dep_v}} p_{EV_v}(t_i) \cdot dt, \quad (33)$$

$$SOC_{EV_v}(t_i) \leq soc_{EV_des_v} \quad \forall t_i = t_{dep_v}, \quad (34)$$

where SOC_{EV} is the SOC of vehicle v , and SOC_{EV_min} and SOC_{EV_max} are the minimum and maximum battery SOC of vehicle v , respectively. The dynamic SOC evolution soc_{EV_v} is given by (33). Similar to the stationary storage, Constraint (29) determines the SOC limit. Additionally, Constraint (30) refers to the absence of an EV, while Constraint (31) assigns the SOC of an EV at its arrival time, requiring it to be greater than the limit specified in Constraint (32). Finally, Constraint (34) refers to the SOC of an EV at its departure time, which should be lower than or equal to the desired SOC of the EV at departure.

3.5. Power Balancing

All the production and consumption should be equal on the DC bus; therefore, an equation for power balancing should be included in the formulation. The power balancing equation [47], where all power signs are assigned positives, is given by (35):

$$p_{PV}(t_i) + p_{S_D}(t_i) + p_{G_S}(t_i) = p_{PVCS}(t_i) + p_{S_C}(t_i) + p_{G_I}(t_i). \quad (35)$$

3.6. Objective Function

The total energy cost C_{total} takes into consideration the cost of the power supplied from the public grid, the profit from the power injected into the public grid, the cost of the stationary storage, the penalty cost in case the EV has not reached the desired SOC at departure, and the cost associated with shedding power from the PV sources. To prevent excessive switching during charging or discharging, a switching penalty C_{SW} is introduced to ensure that the action is completed in the fewest cycles possible. Therefore, the objective function minimizes C_{total} , as given by Equations (36)–(41):

$$\min C_{total} = C_G + C_S + C_{PVS} + C_{EV_penalty} + C_{SW}, \quad (36)$$

$$C_G = \sum_{t_i=t_0}^{t_F} [c_G(t_i) \cdot \Delta t \cdot (-p_{G_I}(t_i) + p_{G_S}(t_i))] \quad (37)$$

$$c_G(t_i) = \begin{cases} c_{G_NH} & \text{for } t \in \text{normal hours} \\ c_{G_PH} & \text{for } t \in \text{normal hours} \end{cases}$$

$$C_S = \sum_{t_i=t_0}^{t_F} [c_S(t_i) \cdot \Delta t \cdot (p_{S_C}(t_i) + p_{S_D}(t_i))], \quad (38)$$

$$C_{PVS} = \sum_{t_i=t_0}^{t_F} [c_{PVS}(t_i) \cdot \Delta t \cdot p_{PVS}(t_i)], \quad (39)$$

$$C_{EV_penalty} = \sum_v^{N_v} [c_{EV_p} \cdot (SOC_{EV_des_v} - SOC_{EV_dep_v}) \cdot E], \quad (40)$$

$$C_{SW} = \sum_{t_i=t_0}^{t_F} \sum_v^{N_v} [c_{SW}(t_i) \cdot (V2G_{SW_v}(t_i) + G2V_{SW_v}(t_i))], \tag{41}$$

where C_G, C_S, C_{PVS} , and $C_{EV_penalty}$ are the public grid, stationary storage, PV shedding, and EV penalty costs, respectively; and $c_G, c_S, c_{PVS}, c_{EV_p}$, and c_{SW} are the public grid, stationary storage, PV shedding, EV penalty, and switching penalty tariffs, respectively. The energy cost optimization problem is formulated to minimize the objective function in (36) with respect to Constraints (8)–(35), determining the decision variables: $p_G, p_S, p_{PV_S}, p_{EV_V}, V2G_{bin_v}, G2V_{bin_v}, V2G_{SW_v}$, and $G2V_{SW_v}$.

4. Simulation Results for PVCS with V2G Service

Several simulation cases are presented to demonstrate the effectiveness of the energy cost optimization method. Finally, the cases with optimization, denoted as “Sim w/ opti”, are compared with the cases without optimization, denoted as “Sim w/o opti”. The “Sim w/o opti” is operated under a simple control scheme based on a storage priority, where k_D is set to one in this operation mode [52]. The optimization problem is solved by CPLEX [53], where CPLEX is a high-performance mathematical programming solver for linear programming, mixed-integer programming, quadratic programming, and convex optimization, developed by IBM. The optimization is performed with 1-min intervals, while the simulation is performed with 1-s intervals. The data for the irradiance and ambient temperature were recorded at 10-s intervals using proper instruments of measurement, and through interpolation, the data are reduced to 1-s intervals.

In this section, two case studies are presented for a PVCS that includes five chargers, with EVs equipped with 50 kWh lithium-ion batteries. The PVCS has 84 PV panels with 28.9 kWp, and the stationary storage has a capacity of 130 Ah, with 288 V providing 37.44 kWh. However, there is no defined power injection limit for the public grid. Table 1 lists the parameters that are used in the following simulation cases for the PVCS with V2G service.

Table 1. Parameter values used in the simulations for the V2G service.

Parameter	Value	Parameter	Value	Parameter	Value
$P_{G_I_max}$	-	SOC_{S_min}	20%	c_{G_NH}	0.1 €/kWh
$P_{G_S_max}$	50 kW	SOC_{S_max}	80%	c_{G_PH}	0.7 €/kWh
P_{S_max}	7 kW	SOC_{EV_min}	20%	c_S	0.01 €/kWh
$P_{EV_fast_max}$	50 kW	SOC_{EV_max}	100%	c_{PVS}	1.2 €/kWh
$P_{EV_aver_max}$	22 kW	SOC_{S_0}	50%	$c_{EV_penalty}$	2.5 €/kWh
$P_{EV_slow_max}$	7 kW	v_S	288 V	c_{SW}	0.05 €
E	50 kWh	C_{Bat}	130 Ah	p_{PV_MPPT}	28.9 kWp

Table 2 presents the EV users’ data and preferences. $SOC_{EV_arr_v}, SOC_{EV_des_v}, t_{arr_v}, M_v$, and V2G participation are generated randomly. $SOC_{EV_arr_v}$ and $SOC_{EV_des_v}$ are generated in the intervals [20%, 50%] and [70%, 100%], respectively. It is assumed that EV battery capacity is capable of handling fast charging.

Table 2. Data and preferences of EV users [43].

EVs	SOC_{EV_arr}	SOC_{EV_des}	t_{arr}	t_{est_ch}	M	V2G
EV1	31%	85%	09:20	03 h 52 min	Slow	Yes
EV2	35%	75%	10:00	0 h 24 min	Fast	No
EV3	50%	80%	12:05	02 h 8 min	Slow	Yes
EV4	25%	78%	13:45	01 h 13 min	Average	No
EV5	29%	72%	14:25	03 h 5 min	Slow	No

Additionally, two scenarios in each study case are taken into consideration:

- Scenario a: during peak periods, EVs discharge at a constant power and then recharge with the same constant charging power as set by the user until departure time;
- Scenario b: during peak periods, EVs discharge at a maximum power of 50 kW and then recharge again with a variable charging power, irrespective of the charging mode selected by the user, to achieve the desired SOC at departure after V2G service.

4.1. Case 1: Sunny Day

For case 1, a day with high irradiance was considered, specifically, 29 June 2019 in Compiègne. The real and predicted PV power are shown in Figure 4, where it can be observed that the predicted PV power is slightly higher than the real PV power and follows the same trend. As a result, this uncertainty has an impact on the optimization results, which will potentially lead to supplying energy from the public grid instead of discharging energy from the stationary storage. In this case, two scenarios are conducted, which involve constant and variable charging/discharging powers.

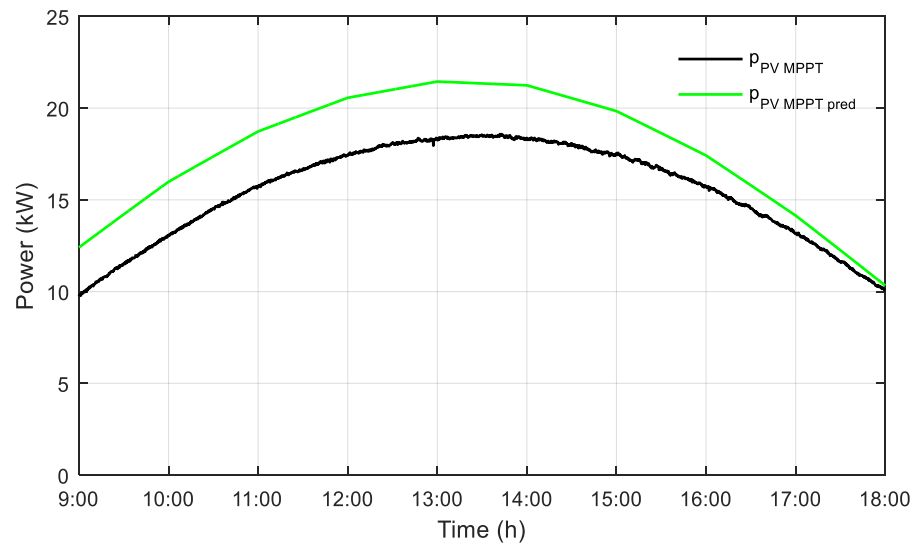


Figure 4. Real PV power $p_{PV\ MPPT}$ and predicted PV power $p_{PV\ MPPT\ pred}$ —29 June 2019.

4.1.1. Scenario a: Constant Power

Figures 5 and 6 show the power and SOC of the EVs with V2G service at constant power with the “Sim w/o opti” and “Sim w/ opti” algorithms, respectively.

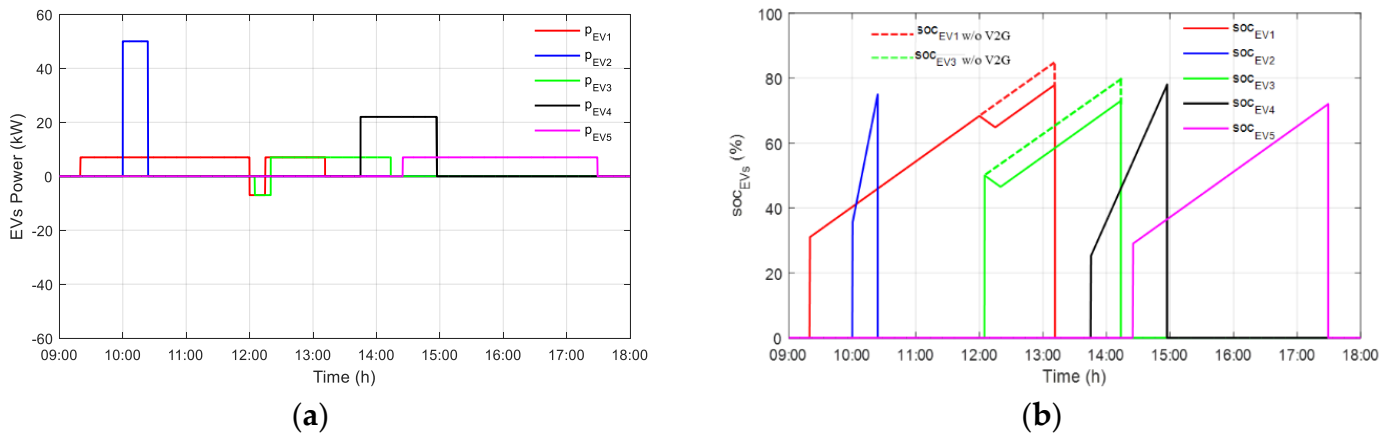


Figure 5. Power (a) and SOC of the EVs (b)—scenario a in “Sim w/o opti”.

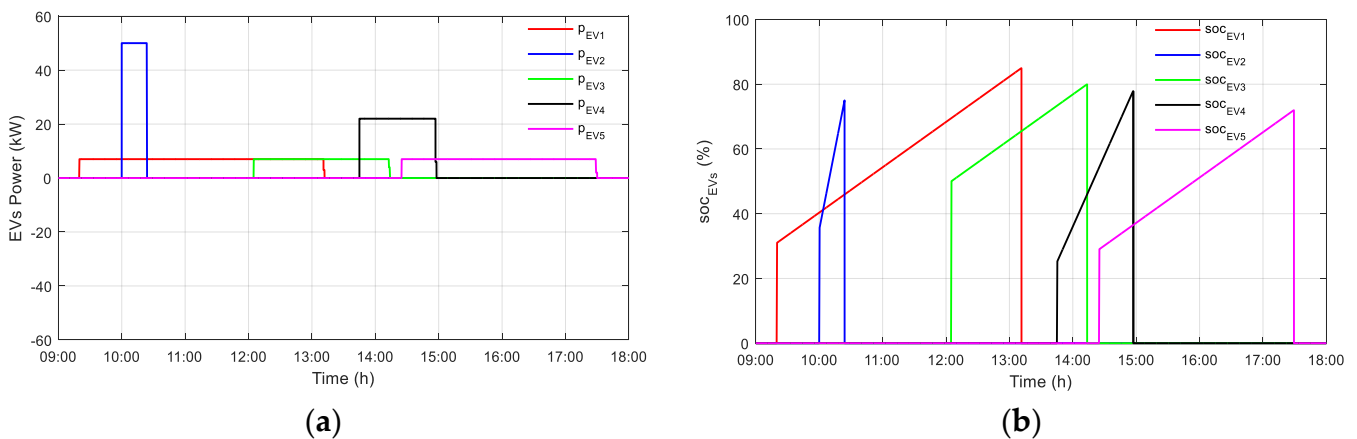


Figure 6. Power (a) and SOC of the EVs (b)—scenario a in “Sim w/ opti”.

Figure 5a shows that EV1 as well EV3 are discharged at peak hours with 7 kW each for 15 min; they are then charged after providing V2G service directly until their departure time with the same constant power. As a result, EV1 and EV3 failed to achieve their desired SOC values at departure. Specifically, EV1 only reached 71% instead of the desired 85%, and EV3 reached 68.33% instead of 80%, as shown in Figure 5b. The dashed points represent the SOC of the EVs that should be reached with respect to user preferences. On the other hand, Figure 6a shows that all the EVs are charging according to user preferences, and the desired SOC at departure is reached even when EV users opt to participate in V2G service, as shown in Figure 6b. However, discharging the EVs is not possible because it would prevent the desired SOC from being achieved, and hence meeting the requirements of EV users is given priority over discharging energy via V2G into the grid.

4.1.2. Scenario b: Variable Power

The power flow of the PVCS with V2G service at variable power with the “Sim w/o opti” and “Sim w/ opti” algorithms is presented in Figure 7, where the predicted PV power is used only to run the optimization, and the real PV power is used in both simulation scenarios.

Figure 7a shows that EV1 as well EV3 are discharged at peak periods for 15 min at 50 kW each, and then they are recharged with the appropriate charging power after V2G service to meet the needs of the users while considering the duration of the remaining parking time. The PVCS operates in storage-priority mode, meaning that any excess PV power is initially used to charge the stationary storage. Once the stationary storage is either full or its maximum charging power is reached, which occurs around 11:00–11:30 and from 15:00 until 18:00, any additional PV power is then injected into the public grid. Furthermore, the public grid provides power when EV2 charges in fast mode and during peak periods when EV1 and EV3 recharge after V2G. Thus, charging EVs during peak periods will increase the energy cost. Sharp variations in power levels might lead to stability issues. To prevent this, Constraint (23) limits steep power variations, which can be seen in Figure 7a’s zoom-in during the peak hour of 12:00 to 13:00. On the other hand, in Figure 7b, EV1 and EV3 are discharged simultaneously during peak periods (serving a total of 100 kW power to the grid), and then each EV recharges after V2G with the optimized power to meet user preferences. EV1 and EV3 are primarily charged by PV power. However, due to uncertainty in the PV power prediction, the public grid may supply power to the EVs between 10:25 and 12:00, although it is not very significant. The injection of power into the public grid is determined by the optimization result to maximize profits in the event of excess PV power, which occurs before 10:00 during V2G service and from 15:00 until 18:00. The power and SOC of the EVs in “Sim w/o opti” and “Sim w/ opti” are shown in Figures 8 and 9, respectively.

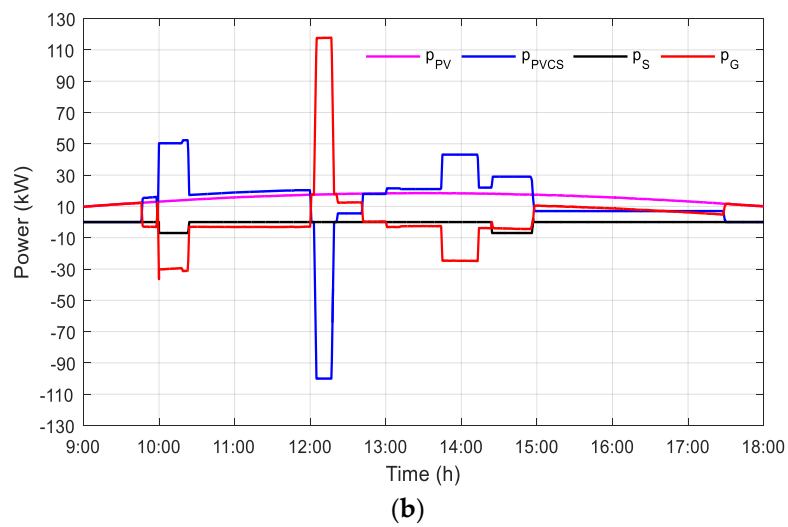
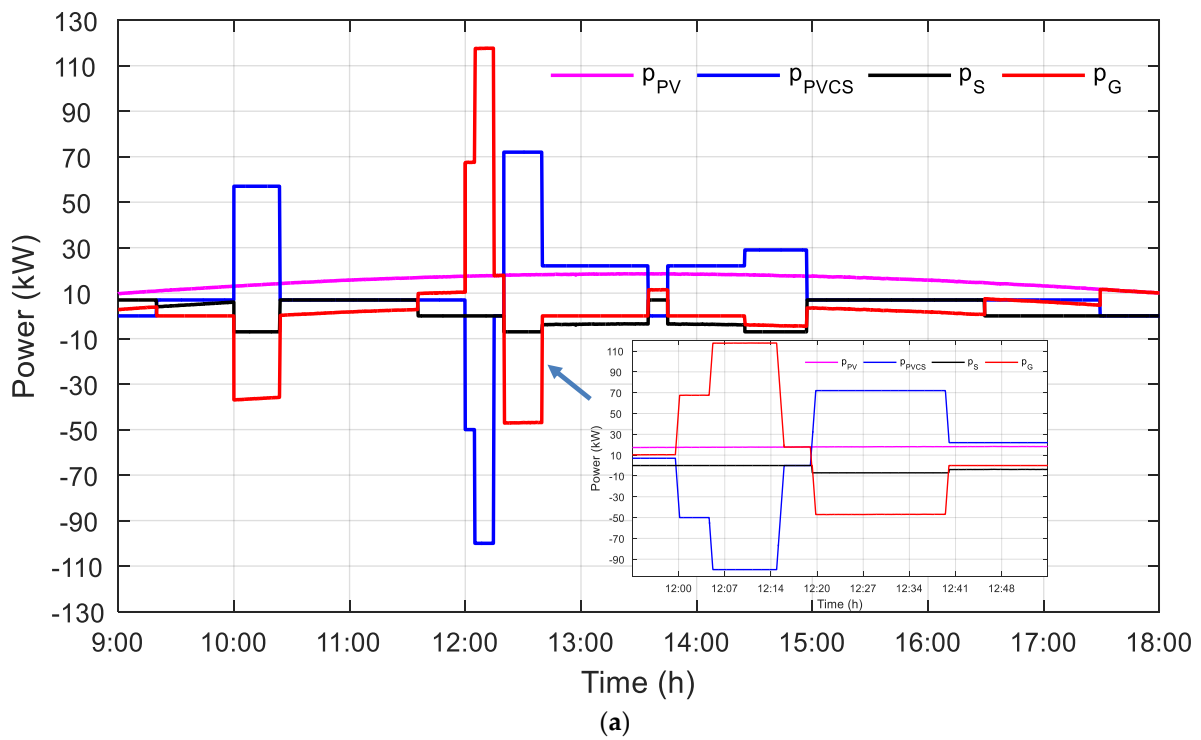


Figure 7. Power flow with V2G service—scenario b (a) in “Sim w/o opti” and (b) in “Sim w/ opti”.

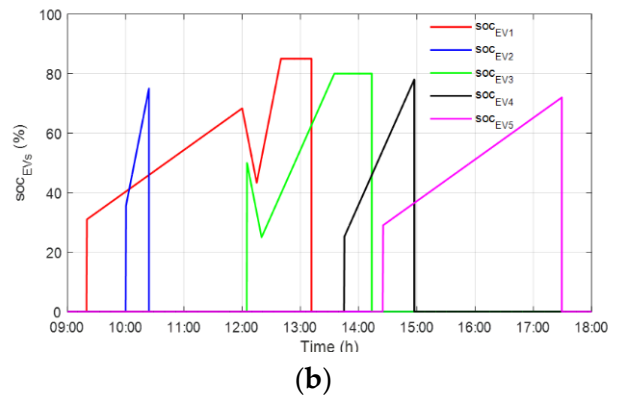
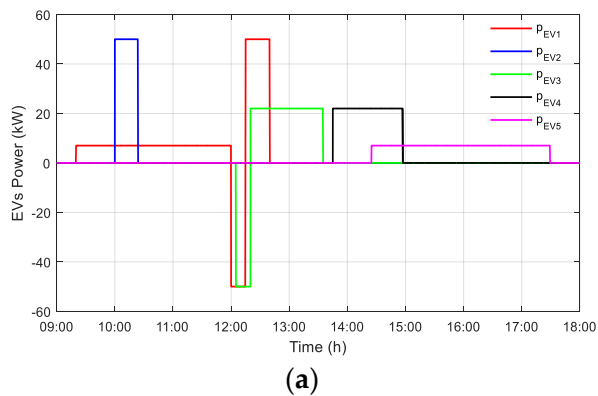


Figure 8. Power (a) and SOC of the EVs (b)—scenario b in “Sim w/o opti”.

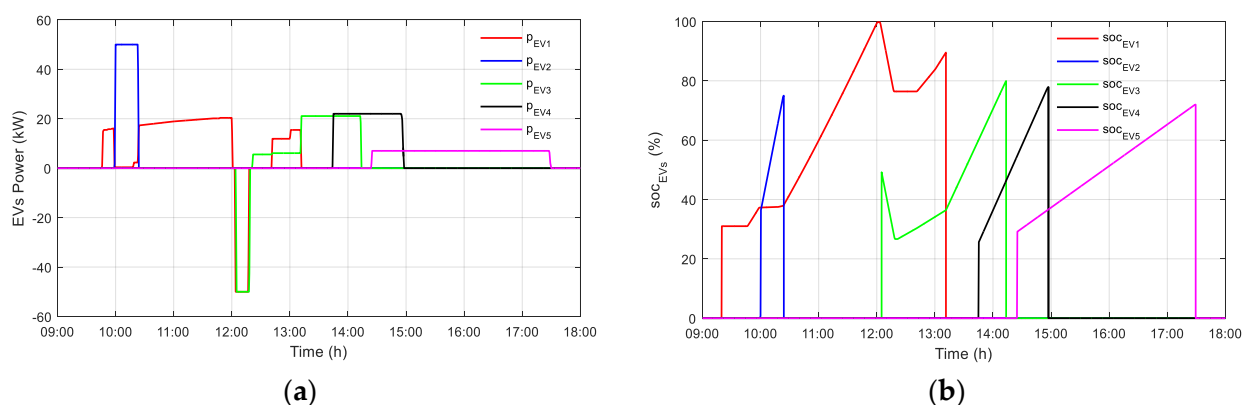


Figure 9. Power (a) and SOC of the EVs (b)—scenario b in “Sim w/ opti”.

Figure 8a shows that EV1 begins discharging at 50 kW and then recharges with 50 kW to reach the desired SOC at the time of departure. The EVs have enough remaining charging time after V2G to recharge with 22 kW. In Figure 9a, the optimized charging/discharging profiles of EV1 and EV3 allow them to participate in V2G service, reach the desired SOC at departure, and satisfy the users with minimization of the cost. When EV2 arrives, the optimization is actualized again, and as a result, EV1’s charging power is dropped to reduce the total power demand because EV2 charges in fast mode. After EV2 leaves, EV1 starts recharging again, which helps to discharge power during peak periods. After providing V2G service, EV1 resumes charging its battery to achieve the desired SOC at the time of departure. In the same way, the optimization is actualized every time a new EV comes to the PVCS, and thus the optimization procedure is realized five times during the day in this case. The power provided to recharge EV1 and EV3 is synchronized with PV power, even during peak periods. Consequently, all EVs have achieved their desired SOC values at the time of departure, as shown in Figures 8b and 9b.

Scenario a, where the charging/discharging power is constant, is proved to be impractical because EVs will never achieve their desired SOC at the time of departure. On the other hand, scenario b proves its feasibility by allowing EVs to recharge with variable power after participating in V2G service, irrespective of their initially selected charging mode, in order to satisfy the EV user. Therefore, only the variable charging/discharging scenario is considered in the following case studies, and the “Sim w/ opti” is compared to the “Sim w/o opti”.

4.2. Case 2: Cloudy Day

For case 2, a cloudy day with high irradiation was considered, specifically, 10 May 2019 in Compiegne. The real and predicted PV powers are shown in Figure 10, where it can be observed that the predicted PV power is slightly higher than the real PV power, and the fluctuations are hard to predict due to hourly provision of forecasts and their inconsistent trends. As a result, these uncertainties have an impact on the optimization results that potentially lead to supplying power from the public grid instead of discharging energy from the stationary storage. In this case, the power flow of the PVCS with V2G service in “Sim w/o opti” and “Sim w/ opti” is shown in Figure 11, where the predicted PV power is used only to run the optimization, and the real PV power is used in both simulation scenarios.

Figure 11a shows that EV1 and EV3 are discharged at peak periods for 15 min with 50 kW each, and they are then recharged after V2G with the appropriate charging power to meet the needs of the users. As the PV power is not very significant and is fluctuating, the stationary storage is discharged to support the charging of EVs. The PVCS operates in storage-priority mode, meaning any excess PV power is initially used to charge the stationary storage. Once the stationary storage is either full or its maximum charging power is reached, which occurs at around 11:30, any additional PV power is injected into the

public grid. However, once the storage is empty, which occurs around 17:00, the public grid supplies power to continue charging the EVs. Furthermore, the public grid supplies power when EV2 charges in fast mode and during peak periods, when EV1 and EV3 recharge after V2G. Therefore, charging EVs during peak periods will increase the energy cost. On the other hand, in Figure 11b, EV1 and EV3 are discharged simultaneously during peak periods (serving total 100 kW power to the grid), and they are then recharged after V2G with optimized power to meet the needs of the users. The power injected into the public grid is defined by the optimization result to maximize profits in the event of excess PV power, which occurs before 09:30, around 11:30 during V2G service, and from 13:15 until 13:45. Figures 12 and 13 show the power and SOC of the EVs for the “Sim w/o opti” and “Sim w/ opti” algorithms, respectively.

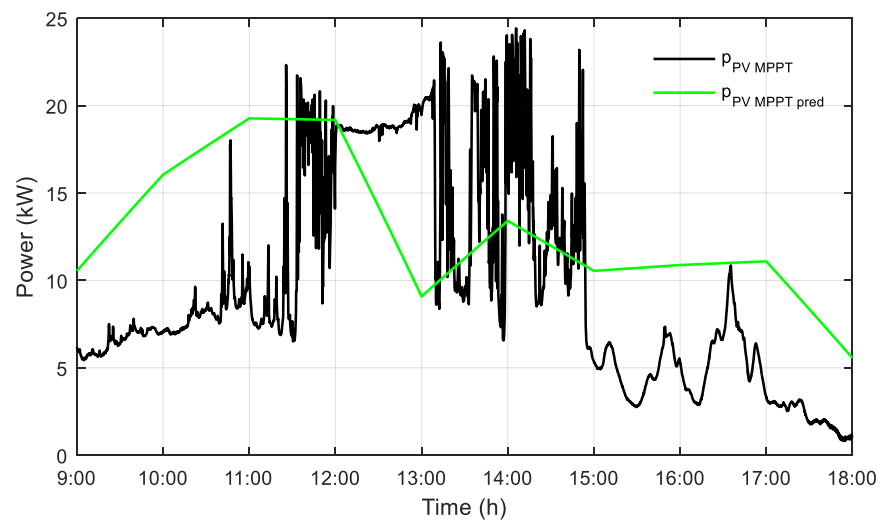


Figure 10. Real PV power p_{PV_MPPT} and predicted PV power $p_{PV_MPPT_pred}$ —10 May 2019.

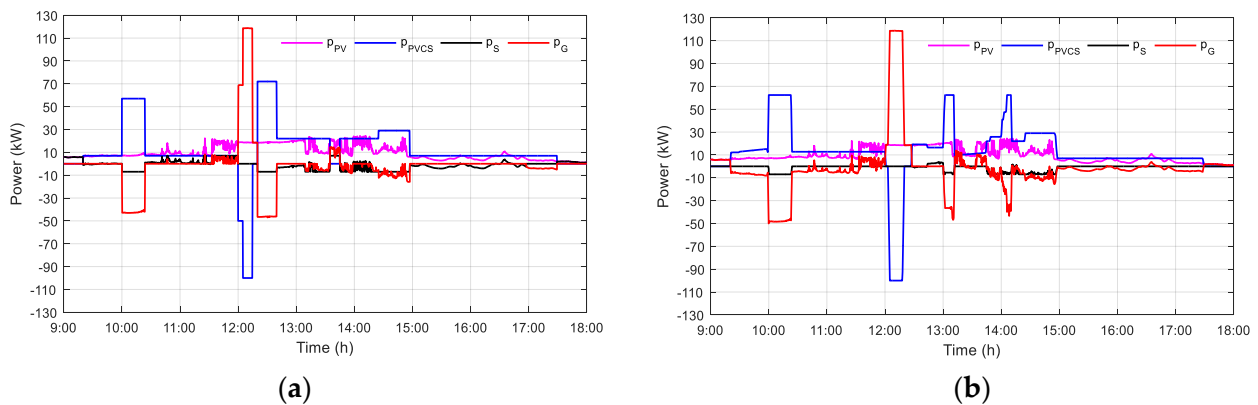


Figure 11. Power flow with V2G service—case 2 (a) in “Sim w/o opti” and (b) in “Sim w/ opti”.

In Figure 12a, similarly to case 1 scenario b under “sim w/o opti”, EV1 and EV3 are discharged at peak periods for 15 min at 50 kW each, and then they continue charging until their departure times to meet the needs of the EV users at 50 kW and 22 kW, respectively. However, in Figure 13a, the charging and discharging profiles of EV1 and EV3 are the optimized profiles that allow them to participate in V2G service, reach the desired SOC at the time of departure, and satisfy the users with the lowest cost. PV power is not very significant; therefore, EV1 keeps charging even when EV2 comes to charge in fast mode. During peak periods, the charging power of EV1 and EV3 is provided by PV sources. Consequently, all EVs have achieved their desired SOC at the time of departure, as shown in Figures 12b and 13b. Figure 14 compares the dynamic SOC of the stationary storage for case 1, scenario b, and case 2.

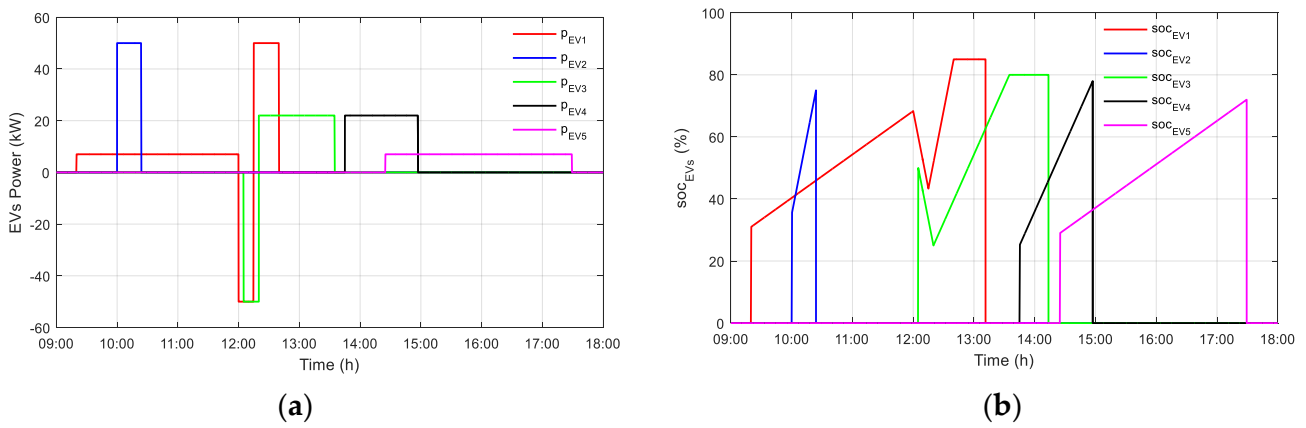


Figure 12. Power (a) and SOC of the EVs (b)—case 2 in “Sim w/o opti”.

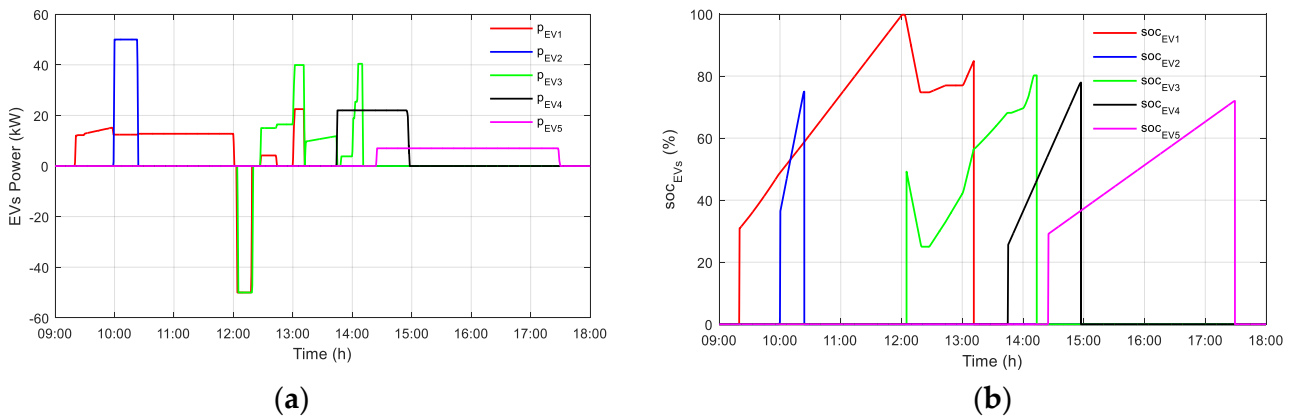


Figure 13. Power (a) and SOC of the EVs (b)—case 2 in “Sim w/ opti”.

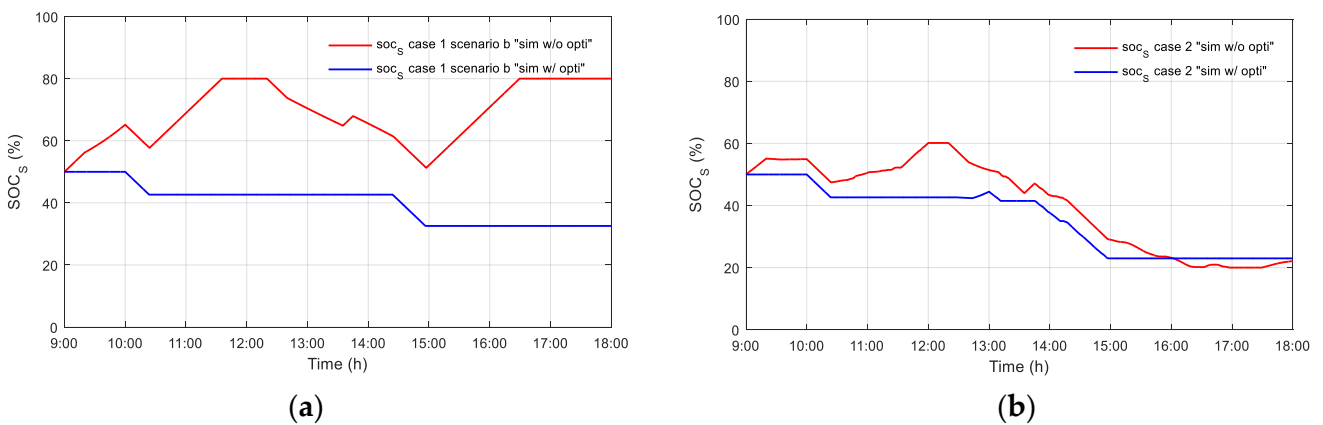


Figure 14. SOC of the stationary storage in (a) case 1, scenario b and (b)—case2.

For Figure 14a, the dynamic SOC of the stationary storage is shown for case 1, where the real PV power is high. In “sim w/o opti”, where the storage priority is applied, the storage is always used for either charging or discharging. The storage becomes full around 11:30 and 16:30, when the charging demand of EVs is not significant. In contrast, in sim w/ opti”, the storage is used only at the moments decided by the optimization algorithm— for example, during peak hours (14:30–15:00) and when the charging demand of EVs is high, such as the case where EV2 charges in fast mode simultaneously with EV1.

On the other hand, Figure 14b shows the dynamic SOC of the stationary storage for case 2, where the real PV is highly fluctuating. In “sim w/o opti”, the storage is always

used for either charging or discharging, but it is never at full capacity and becomes empty around 16:00. In contrast, in “sim w/ opti”, the behavior of the storage is similar to case 1 in “sim w/ opti” and becomes empty at 15:00.

5. Energy Cost Analyses for PV-Powered Charging Station with V2G Service

Table 3 demonstrates the energy injected into the grid for the two case studies. The energy is injected into the grid during V2G, where the EVs’ contribution is significantly greater in the variable charging/discharging power scenario than the constant charging/discharging power scenario. The contribution of EVs is higher than 65% in the variable charging/discharging power scenario. Even in “Sim w/ opti”, the energy share from EVs is similar to that in “Sim w/o opti” and considered significant.

Table 3. Energy injected into the public grid for the different cases.

Operation Case		Energy Injected into the Public Grid during V2G Period					Energy Injected into the Grid during the Day (kWh)
		PV (kWh)	EVs (kWh)	Total Energy during V2G (kWh)	% EV/Total	% PV/Total	
Case 1—constant power scenario	Sim w/o opti	5.88	2.91	8.79	33.10%	66.90%	44.03
	Sim w/ opti	0	0	0	0	0	58.85
Case 1—variable power scenario	Sim w/o opti	5.88	20.83	26.71	77.98%	22.02%	50.95
	Sim w/ opti	5.88	23.33	29.21	79.87%	20.13%	68.34
Case 2—variable power scenario	Sim w/o opti	6.21	20.83	27.04	77.04%	22.96%	30.52
	Sim w/ opti	7.45	25	32.45	77.04%	22.96%	40.91

Furthermore, “Sim w/o opti” and “Sim w/ opti” are compared with an ideal case, which is considered as a reference: “Opti for real conditions”. In this reference case, it is assumed that the real PV MPPT power production and the arrival times of all EVs are known, and hence there will be no uncertainty issues related to forecasting errors. Therefore, the optimization is executed only one time because the arrival times of EVs are considered known in “Opti for real conditions”. The total energy costs of “Sim w/ opti” are closer to the ideal case than “Sim w/o opti” in the two cases, which indicates the effectiveness of the proposed optimization algorithm during different meteorological conditions.

Table 4 presents the energy costs for the case studies. Only in case 1 “Sim w/o opti”, with constant charging/discharging power, is the obtained dissatisfaction cost for EV users positive due to not having the desired SOC at the departure time. In the variable charging/discharging power scenario, the total energy cost is negative, which refers to selling energy to the public grid. Moreover, in “Sim w/ opti” the total energy cost is better due to power injection into the public grid, bringing more profits. In case 1 “Sim w/ opti”, with constant charging/discharging power, the total cost is negative, as there is no penalization due to injecting power to the public grid. However, there is no V2G participation even though the users accept participating to meet the user requirement (minimum SOC of EV) at departure time.

Tables 3 and 4 prove the unfeasibility of the constant charging/discharging scenario, as the energy injected into the public grid from EVs is not significant because they charge/dischARGE with constant power. The total final cost for this scenario is calculated without including the EV penalty cost, which is only included to optimization for modeling the dissatisfaction of the EV users. A high EV penalty indicates that EV users will be dissatisfied due to having low battery energy at departure time, which can cause risks of rejection of enabling V2G services by EV users or even losing clients in the future. The distribution of energy for EVs in “sim w/o opti” and “sim w/ opti” is also assessed in Figures 15 and 16 for case 1b and 2 respectively.

Table 4. Energy costs for the different cases.

Operation Case		Public Grid Cost (c€)	Stationary Storage Cost (c€)	EV Penalty (c€)	Total Cost (c€)
Case 1—constant power scenario	Sim w/o opti	−1106	32	1750 (Dissatisfied client—Risk of losing client)	−1074
	Sim w/ opti	−1247	9	0	−1238
Case 1—variable power scenario	Sim w/o opti	−1006	40	0	−966
	Sim w/ opti	−2942	6	0	−2936
	Opti for real conditions	−4210	10	0	−4200
	Sim w/o opti	−571	28	0	−543
Case 2—variable power scenario	Sim w/ opti	−1745	11	0	−1734
	Opti for real conditions	−2710	11	0	−2699

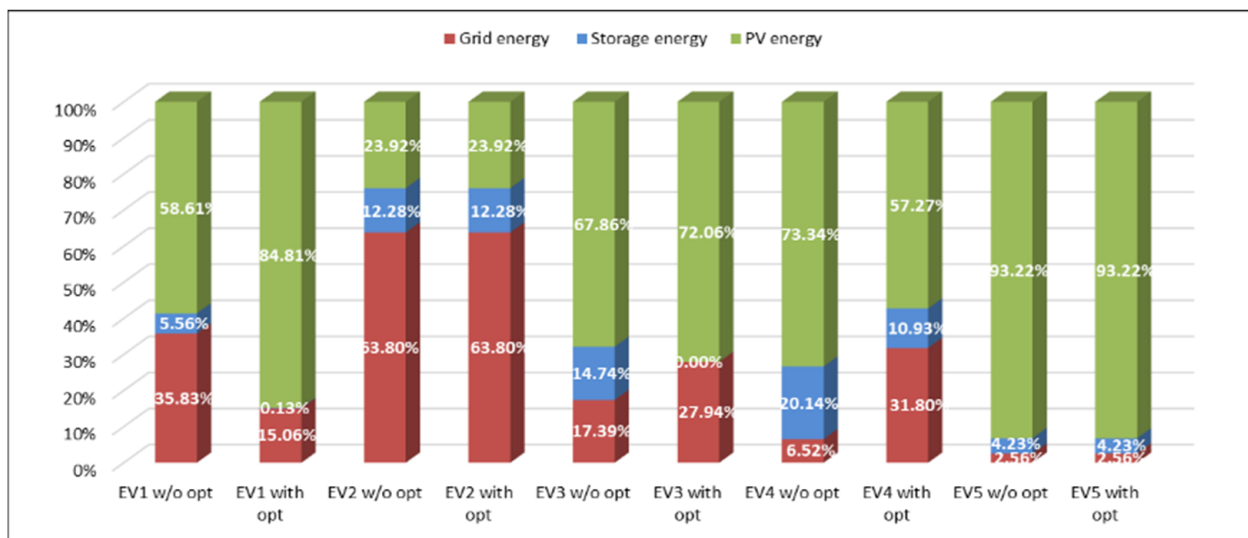


Figure 15. Distribution of energy for EVs in “sim w/o opti” and “sim w/ opti” for case 1b.

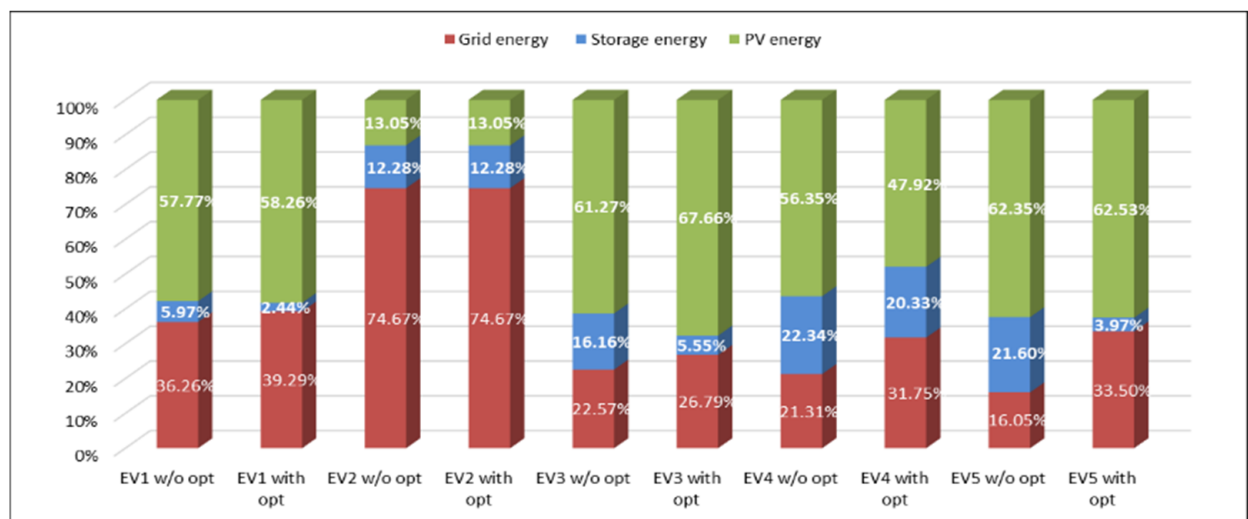


Figure 16. Distribution of energy for EVs in “sim w/o opti” and “sim w/ opti” for case 2.

In Figures 15 and 16, PV sources mainly charge EV1 and EV3. Moreover, in the “sim w/ opti” scenario, the amount of PV energy used for charging EV1 is significantly higher than in the “sim w/o opti” scenario, as shown in case 1. Given that EV2 is charging in fast mode, the primary source of its charging power is the public grid. On the other hand, because EV4 is charged in average mode, it depends on PV and stationary storage energy. Similarly, because EV5 is charged in slow mode, it is mainly charged by PV sources. However, in case 2, EVs require frequent charging from the public grid due to the fluctuation of PV power.

V2G service can improve the energy efficiency of EVs by allowing the EV batteries to be used as a source of energy for the grid during times of high grid demand (and/or high-tariff, low-renewable production) and then recharge from the grid during times of low grid demand (and/or low-tariff, high-renewable production). By providing energy back to the grid, EVs can help balance the electrical load, which can improve the overall efficiency and reliability of the distribution grid. As for the EV users, V2G can provide a way to earn revenue by selling energy stored in their EV batteries back to the grid during peak times. Additionally, the EV batteries can be charged with clean and low-cost renewable resources (e.g., photovoltaics) and can be discharged later to the grid at high-grid-consumption moments via V2G; thus, the electricity grid can use local renewable production more efficiently.

6. Conclusions

In conclusion, a PVCS with energy cost optimization and V2G service can provide a sustainable and cost-effective solution for EV charging/discharging, which can help grid operators by discharging EV batteries via with V2G services, leading to a more efficient system. The focus of the paper is to minimize energy costs, prevent EV penalization and PV shedding, and consider prediction errors in real-time simulations. Additionally, the paper analyzes energy distribution for the system and each EV to gain a better understanding of the system’s functionality. However, there are still some challenges to be addressed in order to optimize the energy cost of the charging station. One of the main challenges is the optimal scheduling of the charging and discharging of the EV batteries to minimize the energy cost and to maximize the charging of EVs with PV power. Furthermore, the cost of implementing and maintaining a PVCS and V2G system can be high, and there is a need to establish standardization and protocols for integration with the existing public grid and communication networks. In addition, the type of an EV can affect the energy cost in the case of V2G because each type of EV has a different battery size, charging and discharging power characteristics, and energy efficiency. Battery EVs have larger batteries with higher power ratings than plug-in EVs and hybrid EVs, which means they can provide more flexibility for charging/discharging operations, and eventually they provide more energy to support the electricity grid. Although V2G operation is possible for FCEVs, the consumption/production of hydrogen can be inefficient compared to battery-based vehicles due to the low efficiency of fuel cells and electrolyzers.

The simulation results show that variable charging and discharging power have major advantages over constant charging/discharging, as no penalization was imposed, and the EV users were satisfied. In addition, optimizing the charging/discharging power is cost-effective because EVs are charged during off-peak hours and discharged during on-peak hours into the public grid, resulting in greater profitability. Furthermore, the energy that EVs inject into the public grid during V2G service is significant, accounting for over 75% of the total energy injected into the public grid during V2G service. The optimization problem is applicable to both private (domestic, work) charging stations and public ones, regardless of their size. By participating in V2G services, EV owners and/or charging station operators can generate revenue and reduce the total energy cost of EV charging, while also providing grid services to improve the reliability and efficiency of the public grid. The HMI allows for the operation of both a single EV and multiple EVs, and the number of EVs that can be operated is only limited by the number of charging terminals. However,

the size of the charging station can affect the applicability of optimization problems for V2G services. For example, a small charging station (e.g., one EV in a residential building) can participate in V2G service to support the electricity grid and earn revenue in return for its services; however, it will have limited power support capacity, and hence it may not be able to provide significant aid individually. In contrast, a large charging station (e.g., 100 EVs in a university parking lot) will have more power capacity, which can enable more significant V2G services for the electricity grid based on its requirements.

For future research, the degradation impact on EV batteries will be studied, as well as the environmental impact. Moreover, more case studies will be conducted to validate the optimization method and demonstrate its feasibility in real-time experimental tests under the concept of power hardware in the loop. Furthermore, annual simulation will be considered where optimization and real-time simulation take into account annual irradiation profiles, temperatures, and EV profiles.

Author Contributions: Conceptualization, S.C.-M., B.C., M.S. and F.L.; methodology, S.C.-M., B.C., M.S. and F.L.; software, S.C.-M.; validation, S.C.-M. and B.C.; formal analysis, S.C.-M. and B.C.; investigation, S.C.-M. and B.C.; resources, S.C.-M.; data curation, S.C.-M.; writing—original draft preparation, S.C.-M.; writing—review and editing, B.C., M.S., and F.L.; visualization, S.C.-M.; supervision, B.C., M.S. and F.L.; project administration, M.S.; funding acquisition, M.S. All authors have read and agreed to the published version of the manuscript.

Funding: This work has been achieved within the framework of the EE4.0 project (Energie Electrique 4.0). EE4.0 is co-financed by the French State and the French Region of Hauts-de-France. This research was also funded by ADEME France, project T-IPV grant number # 2308D0002.

Institutional Review Board Statement: Not applicable.

Informed Consent Statement: Not applicable.

Data Availability Statement: Not applicable.

Conflicts of Interest: The authors declare no conflict of interest.

References

1. Galati, A.; Adamashvili, N.; Crescimanno, M. A Feasibility Analysis on Adopting Electric Vehicles in the Short Food Supply Chain Based on GHG Emissions and Economic Costs Estimations. *Sustain. Prod. Consum.* **2023**, *36*, 49–61. [\[CrossRef\]](#)
2. Yang, Y.; Lu, C.; Liu, H.; Wang, N.; Chen, L.; Wang, C.; Jiang, X.; Ye, C. Optimal Design and Energy Management of Residential Prosumer Community with Photovoltaic Power Generation and Storage for Electric Vehicles. *Sustain. Prod. Consum.* **2022**, *33*, 244–255. [\[CrossRef\]](#)
3. Sierra Rodriguez, A.; de Santana, T.; MacGill, I.; Ekins-Daukes, N.J.; Reinders, A. A Feasibility Study of Solar PV-Powered Electric Cars Using an Interdisciplinary Modeling Approach for the Electricity Balance, CO₂ Emissions, and Economic Aspects: The Cases of The Netherlands, Norway, Brazil, and Australia. *Prog. Photovolt. Res. Appl.* **2020**, *28*, 517–532. [\[CrossRef\]](#)
4. Robisson, B.; Guillemin, S.; Marchadier, L.; Vignal, G.; Mignonac, A. Solar Charging of Electric Vehicles: Experimental Results. *Appl. Sci.* **2022**, *12*, 4523. [\[CrossRef\]](#)
5. Razi, R.; Hajar, K.; Hably, A.; Bacha, S. A User-Friendly Smart Charging Algorithm Based on Energy-Awareness for Different PEV Parking Scenarios. In Proceedings of the 2021 29th Mediterranean Conference on Control and Automation (MED), Puglia, Italy, 22–25 June 2021; pp. 392–397.
6. Tushar, W.; Yuen, C.; Huang, S.; Smith, D.B.; Poor, H.V. Cost Minimization of Charging Stations With Photovoltaics: An Approach With EV Classification. *IEEE Trans. Intell. Transp. Syst.* **2016**, *17*, 156–169. [\[CrossRef\]](#)
7. Yan, D.; Ma, C. Optimal Sizing of A PV Based Electric Vehicle Charging Station Under Uncertainties. In Proceedings of the IECON 2019—45th Annual Conference of the IEEE Industrial Electronics Society, Lisbon, Portugal, 14–17 October 2019; Volume 1, pp. 4310–4315.
8. Chen, Q.; Wang, W.; Wang, H.; Dong, Y.; He, S. Information Gap-Based Coordination Scheme for Active Distribution Network Considering Charging/Discharging Optimization for Electric Vehicles and Demand Response. *Int. J. Electr. Power Energy Syst.* **2023**, *145*, 108652. [\[CrossRef\]](#)
9. Wang, J.; Zhou, N.; Wang, Q.; Liu, H. Hierarchically Coordinated Optimization of Power Distribution Systems with Soft Open Points and Electric Vehicles. *Int. J. Electr. Power Energy Syst.* **2023**, *149*, 109040. [\[CrossRef\]](#)
10. Kempton, W.; Tomić, J. Vehicle-to-Grid Power Implementation: From Stabilizing the Grid to Supporting Large-Scale Renewable Energy. *J. Power Sources* **2005**, *144*, 280–294. [\[CrossRef\]](#)

11. Yoo, Y.; Al-Shawesh, Y.; Tchagang, A. Coordinated Control Strategy and Validation of Vehicle-to-Grid for Frequency Control. *Energies* **2021**, *14*, 2530. [[CrossRef](#)]
12. Habib, S.; Khan, M.M.; Abbas, F.; Sang, L.; Shahid, M.U.; Tang, H. A Comprehensive Study of Implemented International Standards, Technical Challenges, Impacts and Prospects for Electric Vehicles. *IEEE Access* **2018**, *6*, 13866–13890. [[CrossRef](#)]
13. Mortaz, E.; Valenzuela, J. Optimizing the Size of a V2G Parking Deck in a Microgrid. *Int. J. Electr. Power Energy Syst.* **2018**, *97*, 28–39. [[CrossRef](#)]
14. Fan, P.; Ke, S.; Yang, J.; Li, R.; Li, Y.; Yang, S.; Liang, J.; Fan, H.; Li, T. A Load Frequency Coordinated Control Strategy for Multimicrogrids with V2G Based on Improved MA-DDPG. *Int. J. Electr. Power Energy Syst.* **2023**, *146*, 108765. [[CrossRef](#)]
15. Habib, S.; Kamran, M.; Rashid, U. Impact Analysis of Vehicle-to-Grid Technology and Charging Strategies of Electric Vehicles on Distribution Networks—A Review. *J. Power Sources* **2015**, *277*, 205–214. [[CrossRef](#)]
16. Noel, L.; Zarazua de Rubens, G.; Kester, J.; Sovacool, B.K. *Vehicle-to-Grid: A Sociotechnical Transition Beyond Electric Mobility*; Springer International Publishing: Cham, Switzerland, 2019; ISBN 978-3-030-04863-1.
17. Saldaña, G.; San Martin, J.I.; Zamora, I.; Asensio, F.J.; Oñederra, O. Electric Vehicle into the Grid: Charging Methodologies Aimed at Providing Ancillary Services Considering Battery Degradation. *Energies* **2019**, *12*, 2443. [[CrossRef](#)]
18. Ravi, S.S.; Aziz, M. Utilization of Electric Vehicles for Vehicle-to-Grid Services: Progress and Perspectives. *Energies* **2022**, *15*, 589. [[CrossRef](#)]
19. Huber, D.; De Clerck, Q.; De Cauwer, C.; Sapountzoglou, N.; Coosemans, T.; Messagie, M. Vehicle to Grid Impacts on the Total Cost of Ownership for Electric Vehicle Drivers. *World Electr. Veh. J.* **2021**, *12*, 236. [[CrossRef](#)]
20. Qi, S.; Lin, Z.; Song, J.; Lin, X.; Liu, Y.; Ni, M.; Wang, B. Research on Charging–Discharging Operation Strategy for Electric Vehicles Based on Different Trip Patterns for Various City Types in China. *World Electr. Veh. J.* **2022**, *13*, 7. [[CrossRef](#)]
21. Shipman, R.; Waldron, J.; Naylor, S.; Pinchin, J.; Rodrigues, L.; Gillott, M. Where Will You Park? Predicting Vehicle Locations for Vehicle-to-Grid. *Energies* **2020**, *13*, 1933. [[CrossRef](#)]
22. Han, H.-S.; Oh, E.; Son, S.-Y. Study on EV Charging Peak Reduction with V2G Utilizing Idle Charging Stations: The Jeju Island Case. *Energies* **2018**, *11*, 1651. [[CrossRef](#)]
23. Liu, L.; Xie, F.; Huang, Z.; Wang, M. Multi-Objective Coordinated Optimal Allocation of DG and EVCSs Based on the V2G Mode. *Processes* **2021**, *9*, 18. [[CrossRef](#)]
24. Di Natale, L.; Funk, L.; Rüdüsüli, M.; Svetozarevic, B.; Pareschi, G.; Heer, P.; Sansavini, G. The Potential of Vehicle-to-Grid to Support the Energy Transition: A Case Study on Switzerland. *Energies* **2021**, *14*, 4812. [[CrossRef](#)]
25. Luo, L.; Wu, Z.; Gu, W.; Huang, H.; Gao, S.; Han, J. Coordinated Allocation of Distributed Generation Resources and Electric Vehicle Charging Stations in Distribution Systems with Vehicle-to-Grid Interaction. *Energy* **2020**, *192*, 116631. [[CrossRef](#)]
26. Mehrjerdi, H.; Rakhshani, E. Vehicle-to-Grid Technology for Cost Reduction and Uncertainty Management Integrated with Solar Power. *J. Clean. Prod.* **2019**, *229*, 463–469. [[CrossRef](#)]
27. Amamra, S.-A.; Marco, J. Vehicle-to-Grid Aggregator to Support Power Grid and Reduce Electric Vehicle Charging Cost. *IEEE Access* **2019**, *7*, 178528–178538. [[CrossRef](#)]
28. AbuElrub, A.; Hamed, F.; Saadeh, O. Microgrid Integrated Electric Vehicle Charging Algorithm with Photovoltaic Generation. *J. Energy Storage* **2020**, *32*, 101858. [[CrossRef](#)]
29. Steffen, T.; Fly, A.; Mitchell, W. Optimal Electric Vehicle Charging Considering the Effects of a Financial Incentive on Battery Ageing. *Energies* **2020**, *13*, 4742. [[CrossRef](#)]
30. Wang, D.; Sechilariu, M.; Locment, F. PV-Powered Charging Station for Electric Vehicles: Power Management with Integrated V2G. *Appl. Sci.* **2020**, *10*, 6500. [[CrossRef](#)]
31. Jang, Y.; Sun, Z.; Ji, S.; Lee, C.; Jeong, D.; Choung, S.; Bae, S. Grid-Connected Inverter for a PV-Powered Electric Vehicle Charging Station to Enhance the Stability of a Microgrid. *Sustainability* **2021**, *13*, 14022. [[CrossRef](#)]
32. Wang, Y.; Gladwin, D. Power Management Analysis of a Photovoltaic and Battery Energy Storage-Based Smart Electrical Car Park Providing Ancillary Grid Services. *Energies* **2021**, *14*, 8433. [[CrossRef](#)]
33. Abronzini, U.; Attaianese, C.; D’Arpino, M.; Di Monaco, M.; Tomasso, G. Cost Minimization Energy Control Including Battery Aging for Multi-Source EV Charging Station. *Electronics* **2019**, *8*, 31. [[CrossRef](#)]
34. Ul-Haq, A.; Cecati, C.; Al-Amman, E.A. Modeling of a Photovoltaic-Powered Electric Vehicle Charging Station with Vehicle-to-Grid Implementation. *Energies* **2017**, *10*, 4. [[CrossRef](#)]
35. Mumtaz, S.; Ali, S.; Ahmad, S.; Khan, L.; Hassan, S.Z.; Kamal, T. Energy Management and Control of Plug-In Hybrid Electric Vehicle Charging Stations in a Grid-Connected Hybrid Power System. *Energies* **2017**, *10*, 1923. [[CrossRef](#)]
36. Onishi, V.C.; Antunes, C.H.; Trovão, J.P.F. Optimal Energy and Reserve Market Management in Renewable Microgrid-PEVs Parking Lot Systems: V2G, Demand Response and Sustainability Costs. *Energies* **2020**, *13*, 1884. [[CrossRef](#)]
37. Aluisio, B.; Conserva, A.; Dicorato, M.; Forte, G.; Trovato, M. Optimal Operation Planning of V2G-Equipped Microgrid in the Presence of EV Aggregator. *Electr. Power Syst. Res.* **2017**, *152*, 295–305. [[CrossRef](#)]
38. Zhou, T.; Sun, W. Research on Multi-Objective Optimisation Coordination for Large-Scale V2G. *IET Renew. Power Gener.* **2020**, *14*, 445–453. [[CrossRef](#)]
39. Modarresi Ghazvini, A.; Olamaei, J. Optimal Sizing of Autonomous Hybrid PV System with Considerations for V2G Parking Lot as Controllable Load Based on a Heuristic Optimization Algorithm. *Sol. Energy* **2019**, *184*, 30–39. [[CrossRef](#)]

40. Vermeer, W.; Chandra Mouli, G.R.; Bauer, P. Real-Time Building Smart Charging System Based on PV Forecast and Li-Ion Battery Degradation. *Energies* **2020**, *13*, 3415. [[CrossRef](#)]
41. Shi, R.; Li, S.; Zhang, P.; Lee, K.Y. Integration of Renewable Energy Sources and Electric Vehicles in V2G Network with Adjustable Robust Optimization. *Renew. Energy* **2020**, *153*, 1067–1080. [[CrossRef](#)]
42. Kajanova, M.; Bracinik, P. The Vehicle-to-Grid Concept with Respect to the Preferences of Electric Vehicle Drivers and Charging Station Operators. *Appl. Sci.* **2022**, *12*, 5476. [[CrossRef](#)]
43. Cheikh-Mohamad, S.; Sechilariu, M.; Locment, F. PV-Powered Charging Station: Energy Management with V2G Operation and Energy Cost Analysis. In Proceedings of the 2022 7th International Conference on Smart and Sustainable Technologies (SpliTech), Split, Croatia, 5–8 July 2022; pp. 1–6.
44. Cheikh-Mohamad, S.; Sechilariu, M.; Locment, F. Real-Time Power Management Including an Optimization Problem for PV-Powered Electric Vehicle Charging Stations. *Appl. Sci.* **2022**, *12*, 4323. [[CrossRef](#)]
45. Cheikh-Mohamad, S.; Sechilariu, M.; Locment, F. PV-Powered Charging Station: Energy Management and Cost Optimization. In Proceedings of the 2021 IEEE 30th International Symposium on Industrial Electronics (ISIE), Kyoto, Japan, 20–23 June 2021; pp. 1–6.
46. Sechilariu, M.; Molines, N.; Richard, G.; Martell-Flores, H.; Locment, F.; Baert, J. Electromobility Framework Study: Infrastructure and Urban Planning for EV Charging Station Empowered by PV-Based Microgrid. *IET Electr. Syst. Transp.* **2019**, *9*, 176–185. [[CrossRef](#)]
47. Sechilariu, M.; Locment, F. Direct Current Microgrid Power Modeling and Control. In *Urban DC Microgrid*; Elsevier: Amsterdam, The Netherlands, 2016; pp. 133–170. ISBN 978-0-12-803736-2.
48. Sechilariu, M.; Locment, F. Experimental Evaluation of Urban Direct Current Microgrid. In *Urban DC Microgrid*; Elsevier: Amsterdam, The Netherlands, 2016; pp. 209–250. ISBN 978-0-12-803736-2.
49. Montaña-Salcedo, C.E.; Sechilariu, M.; Locment, F. Human-System Interfaces for PV-Powered Electric Vehicles Charging Station. In Proceedings of the 2021 IEEE 30th International Symposium on Industrial Electronics (ISIE), Kyoto, Japan, 20–23 June 2021; pp. 1–6.
50. Marra, F.; Yang, G.Y.; Træholt, C.; Larsen, E.; Rasmussen, C.N.; You, S. Demand Profile Study of Battery Electric Vehicle under Different Charging Options. In Proceedings of the 2012 IEEE Power and Energy Society General Meeting, San Diego, CA, USA, 22–26 July 2012; pp. 1–7.
51. Sechilariu, M.; Locment, F. Backup Power Resources for Microgrid. In *Urban DC Microgrid*; Elsevier: Amsterdam, The Netherlands, 2016; pp. 93–132. ISBN 978-0-12-803736-2.
52. Wang, D.; Locment, F.; Sechilariu, M. Modelling, Simulation, and Management Strategy of an Electric Vehicle Charging Station Based on a DC Microgrid. *Appl. Sci.* **2020**, *10*, 2053. [[CrossRef](#)]
53. ILOG CPLEX Optimization Studio—Overview. Available online: <https://www.ibm.com/products/ilog-cplex-optimization-studio> (accessed on 16 March 2022).

Disclaimer/Publisher’s Note: The statements, opinions and data contained in all publications are solely those of the individual author(s) and contributor(s) and not of MDPI and/or the editor(s). MDPI and/or the editor(s) disclaim responsibility for any injury to people or property resulting from any ideas, methods, instructions or products referred to in the content.